JOURNAL OF MATERIALS SCIENCE 29 (1994) 2761–2766

# Nucleation and growth mechanism of diamond during hot-filament chemical vapour deposition

J. SINGH*
*NASA — George C. Marchall Space Flight Center, Huntsville, Alabama 35812, USA*

High-resolution transmission electron microscopy (HRTEM) was employed to study the nucleation and subsequent growth mechanism of crystalline diamond grown on copper TEM grids by the hot-filament chemical vapour deposition process. The HRTEM revealed direct evidence for the formation of a diamond-like amorphous carbon layer 8–14 nm thick, in which small diamond microcrystallites about 2–5 nm across were embedded. These diamond microcrystallites were formed as a result of direct transformation of the diamond-like carbon into diamond. Large diamond crystallites were observed to grow from these microcrystallites. The diamond surface was found to be non-uniform. It is envisaged that the diamond microcrystallites present in the amorphous, diamond-like carbon layer provide nucleation sites on which the large diamond crystallites grew. A mechanism of diamond growth has been proposed, based on the experimental findings, and is consistent with available theoretical models and numerous experimental observations reported in the literature.

## 1. Introduction

Diamond thin films have been deposited using a variety of chemical vapour deposition techniques which include hot filament [1], microwave chemical vapour deposition [2], RF plasma [3], and DC jet [4]. The diamond films on heterosubstrates are generally of a polycrystalline nature. Nucleation of diamond phase on a given substrate is a strong function of substrate conditions, including the surface preparation procedure. It has been found that scratching the substrate with diamond grit is quite effective in enhancing the density of diamond nuclei. The scratching results in diamond residual particles which provide seeds for diamond growth [5]. For these seeds to be effective, they must be stable at the growth temperature, i.e. solubility and diffusivity of carbon into the substrate should not lead to disintegration of diamond particles. In the absence of pre-existing diamond particles, the mechanism of diamond nucleation is unclear, and has intrigued many researchers in the field.

This investigation aimed to explore the mechanism of diamond nucleation on heterosubstrates. In this study, we have adopted a novel technique in which diamond is grown on transmission electron microscope (TEM) grids which can be directly examined in the microscope as a function of duration of chemical vapour deposition growth. Based upon the TEM and scanning electron microscope (SEM) observations of these specimens as a function of growth conditions during hot-filament chemical vapour deposition (HFCVD), a mechanism is proposed for the nucleation and subsequent growth of diamond.

## 2. Experimental procedure

The HFCVD process was used to deposit diamond crystallites on copper (75 mesh) grids. The TEM grids were placed on an alumina substrate. The sample was heated by radiation of a hot tungsten filament, as well as by a heat lamp under the specimen holder. The filament, with a temperature of about 1950 °C as measured by an optical pyrometer, was positioned 8 mm above the substrate. A pre-mixed gas flow of $CH_4 + H_2$ was directed on to the substrate by a jet above the filament source. The gas flow rate was measured by a flowmeter in terms of standard cubic-centimetres per minute (SCCM) and ambient gas pressure was controlled by a mechanical valve. The system was continuously pumped during deposition by a mechanical pump. The substrate temperature was about 850 °C, the gas ratio ($H_2$:$CH_4$) used was 100:1, and the total gas pressure was maintained at about 20 torr. The deposition time was $\sim$ 4 h. Two sets of samples were prepared for microstructural characterization: (i) after growing the diamond thin films on grids, the system was quickly shut down and the sample was immediately examined in the HRTEM; (ii) after the diamond thin film deposition on the substrate was terminated, the methane gas flow was shut off and hydrogen gas was continued at the same deposition temperature for $\sim$ 30 min. The main objective was to determine whether atomic hydrogen exposure can affect the surface properties or growth of diamond thin films. The deposited films were characterized by SEM (Jeol JSM 6400FE with a cold-field emission gun) and by high resolution TEM (TOPCON 002B operated at 200 kV).

## 3. Results

Fig. 1 shows SEM micrographs taken at two different magnifications of copper grids, containing diamond

*Present address: Applied Research Laboratory, Penn State University, State College, PA 16804.

0022–2461  

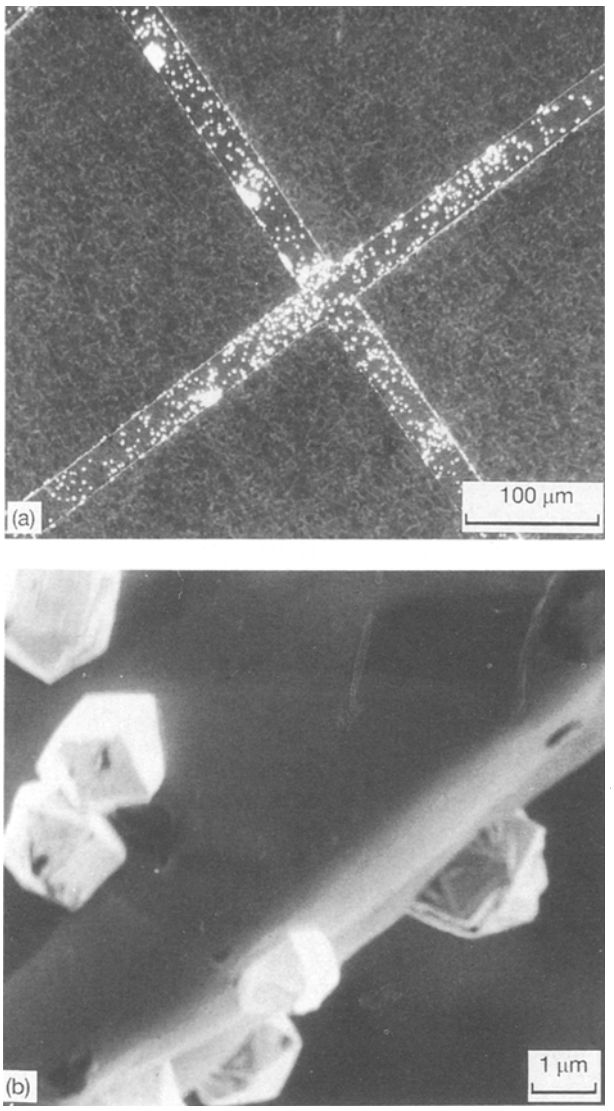


*Figure 1* SEM micrographs of diamond thin film deposited on the TEM grid, showing faceted morphology on the side of the copper grid.

crystallites on the top as well as on the sides of the grid. The diamond crystallites exhibited hexagonal and cubo-octahedron morphology. These grids were used directly in a HRTEM to study the nucleation mechanism of diamond. Fig. 2 is a low-magnification TEM micrograph showing faceted growth of diamond crystallites at the edge of a TEM grid. Fig. 3 is a HRTEM micrograph showing the growth of a diamond crystal at the edge of a TEM grid. The phase between the diamond and grid appeared to be amorphous, as marked by the arrow in Fig. 3. Diffraction analysis of this amorphous phase could not be conducted as it was very close to the grid. The diamond crystal did not have completely faceted boundaries. The BC boundary appeared to be curved, whereas the AB and CD boundaries were sharp and faceted (Fig. 3). The lattice planes were parallel to the faceted boundaries of the crystal, i.e. CD or AB, and corresponded to the $\{1\,1\,1\}$ planes of diamond. The lattice planes of the diamond crystal were found to terminate at the amorphous/diamond interface. Fig. 4 is an HRTEM micrograph of the diamond crystal showing cross lattice fringes, i.e. $\{1\,1\,1\}$ planes of diamond that are clearly resolved. The amorphous-to-crystalline interface was found to be non-uniform. In the amorphous layer, embedded microcrystallites of much smaller size (2–3 nm) were found. The thickness of the amorphous layer was determined to be about 8–10 nm, and the surface was non-uniform. The presence of such microcrystallites was also observed between two diamond crystallites (A and B), as shown by arrows in Fig. 5.

Fig. 6 is a TEM micrograph from another specimen showing the growth of secondary diamond crystallites on the primary faceted diamond crystal, as indicated by the arrow. The average size of the secondary crystallites was determined to be about 0.1 μm. The edge of protruding secondary diamond crystallites was thin enough for microstructural evaluations. At the edge of primary and secondary diamond crystallites, the amorphous layer was observed around the diamond crystal, as shown by arrows in Fig. 7. The

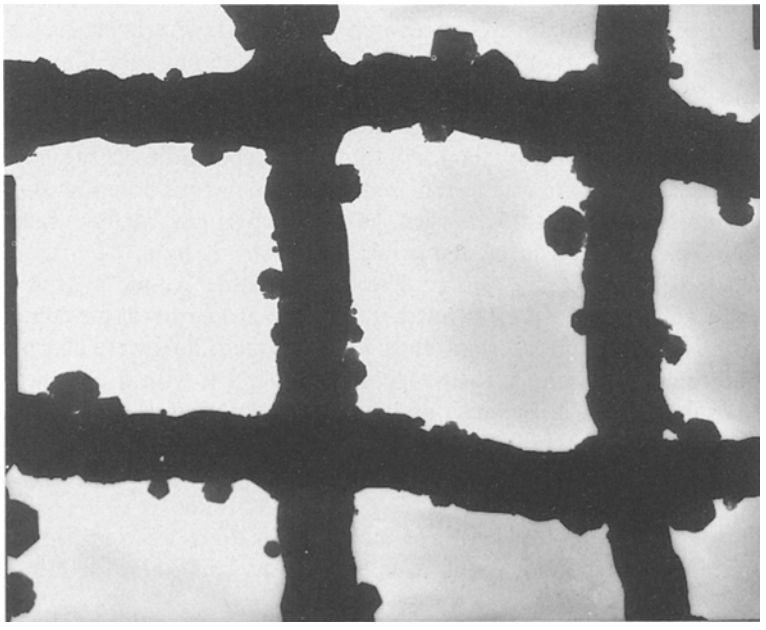

*Figure 2* Low-magnification TEM micrograph showing the growth of diamond crystallites at the edge of the TEM grid.

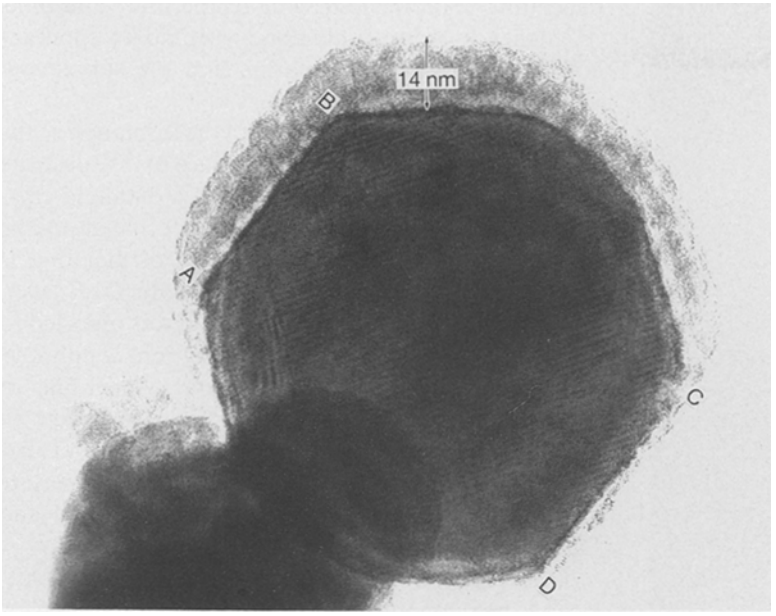


*Figure 3* HRTEM micrograph of the faceted diamond crystal, showing ~ 10-nm-thick amorphous layer around the diamond crystal.

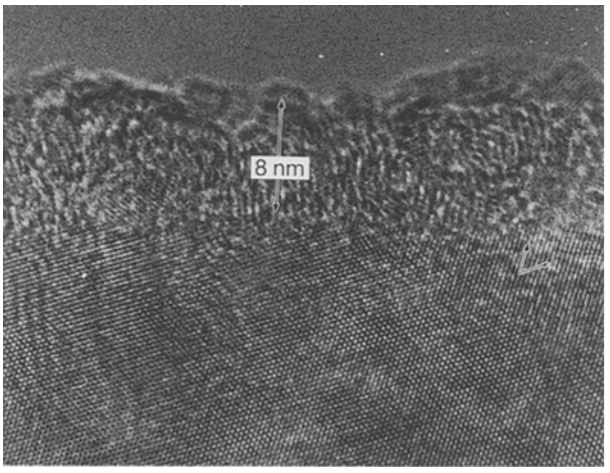


*Figure 4* HRTEM micrograph showing the non-uniform amorphous and crystalline interface.

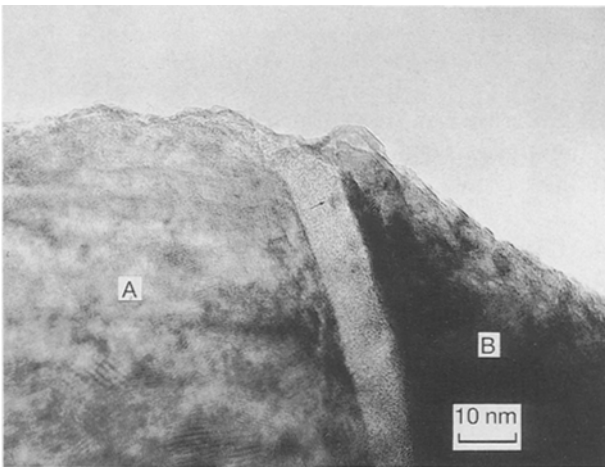


*Figure 5* HRTEM micrograph showing the microcrystallite region in the amorphous phase (arrow).

secondary diamond crystallites (A) appeared to be embedded in the amorphous layer on the surfaces of the primary diamond crystal (B). The average thickness of the amorphous layer around the secondary diamond was determined to be about 6 nm. In addition, the amorphous layer was found to be non-uniform. The interface between the primary and secondary diamond crystallites could not be resolved as the interface was too thick. However, the thickness of the amorphous layer on the primary diamond (near the secondary diamond) was about 15–18 nm. It is interesting to note that the primary diamond crystal had a faceted nature, whereas the secondary diamond crystallites were still non-faceted, i.e. secondary diamond crystallites were hemispherical and embedded in the amorphous layer (Figs 6 and 7). The {1 1 1} lattice planes of the diamond were clearly resolved, and the planes terminated at the amorphous–diamond crystal interface. The spacing between these lattice planes corresponded to the {1 1 1} lattice planes of the diamond crystal. The diamond microcrystallites were also found to be embedded in the amorphous layer, as shown by the arrows in Fig. 7. These results indicate that the part of the diamond-like carbon

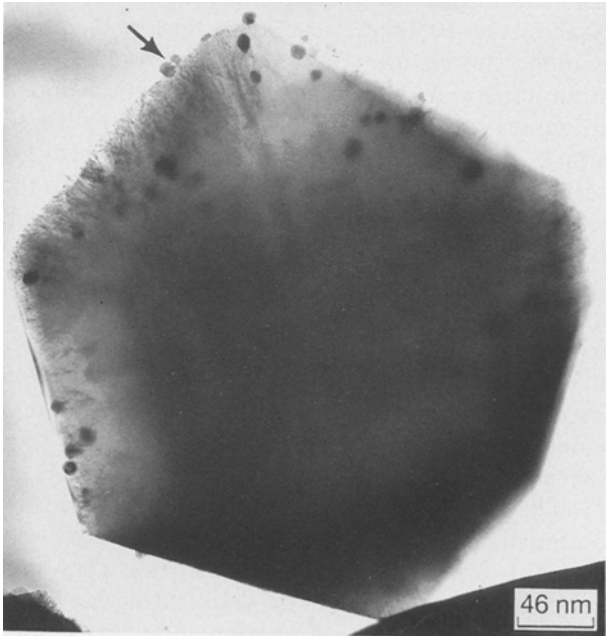


*Figure 6* Low-magnification TEM micrograph showing growth of secondary diamond crystallites on the primary diamond crystal.

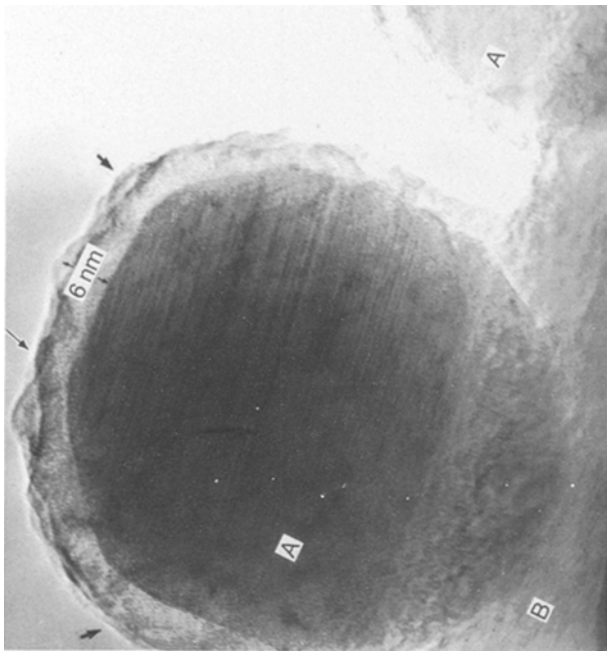


*Figure 7* HRTEM micrograph showing growth of secondary diamond crystallites on the primary diamond crystal.

(DLC) layer was transformed into a crystalline diamond phase. The large diamond crystallites appeared to have grown from these 2–3 nm microcrystallites.

## 4. Discussion

According to Fedoseev & Derjaguin [6] and Frenklach & Spear [7], diamond, DLC and graphite can be formed from various hydrocarbons under different experimental conditions. In the early stage of synthesis of diamond, when the substrate is not covered with diamond, carbon clusters are formed on the substrate surface as a result of numerous chemical reactions. The majority of carbon clusters have thermodynamically stable graphite and amorphous structures, but metastable diamond structures are also formed due to thermodynamic fluctuations. Since the chemical etching reaction rate of graphite with atomic hydrogen is about 30–50 times faster than that of diamond, graphite clusters are removed rapidly from the substrate surface. As a result, only clusters with diamond structures stay and grow. Further, atomic hydrogen attacks the unsaturated $sp^1$ and $sp^2$ bonds between carbon atoms in the clusters to convert them into the tetrahedral $sp^3$ bonds [8]. Thus the atomic hydrogen facilitates the formation of diamond clusters with only $sp^3$ bonds, suppressing other forms of clusters having unsaturated bonds. The growth mechanism of diamond clusters is perhaps purely chemical [8].

Liu *et al.* [9] reported that critical doses of ion implantation created amorphous layers on the diamond surface at liquid nitrogen temperature (77 K). On subsequent rapid thermal annealing (RTA) at 1100 °C for 2 min, the amorphous layer recrystallized on the diamond surface. The recrystallized layer was reported to have diamond characteristics. They suggested that the regrowth of the diamond surface was a result of solid-state transformation of the amorphous phase into diamond. In addition, the regrowth of the diamond layer was reported to be an epitaxial growth, depending upon the annealing temperature and time. At higher ion doses, diamond graphitizes spontaneously during the implantation and the subsequent annealing is not required.

Ravi *et al.* [10] have considered the formation of the amorphous layer (DLC) on the surface of the substrate before the nucleation and growth of a diamond crystal. They reported that the dramatic change in the density and the growth morphology of diamond is influenced by the nucleation density of the DLC layer. The morphology of a diamond crystal was reported to be a strong function of the nucleation conditions, rather than of gas-solid interactions. According to Frenklach and Spear [7], atomic hydrogen plays an important role in the nucleation and growth of diamond. More specifically, its super equilibrium state has a strong promoting effect on the diamond and DLC growth.

The existence of the amorphous phase on the surface of the diamond crystallites has been reported by various investigators. Tuinsta & Koenig [11] and Nemanich *et al.* [12, 13] have done extensive micro-Raman analyses on the growth of diamond thin films at different diamond growth environments. They reported two distinct Raman peaks, at 1332 $cm^{-1}$ for diamond and 1580 $cm^{-1}$ for graphite. Additional features were observed at 1140 $cm^{-1}$, which were attributed to the disorder or microcrystalline domains having $sp^3$-bonded carbon [14, 15]. The disordered $sp^3$-bonded carbon was reported to be a precursor for the formation of diamond. The thickness of the precursor layer around the diamond was reported to be of the order of 6 nm. These findings have been confirmed by Solin & Kobliska [15] and Shroder *et al.* [16]. In the present study, the precursor layer around the diamond crystallites was also observed, which was determined to be of the order of 10–14 nm. When specimens were exposed to a hydrogen plasma for 10 min after the methane was shut down, the size of domain around the diamond was found to be reduced to about 6 nm. This was due to etching of the diamond surface by the hydrogen termination.

The crystallization of the amorphous phase can be explained on the basis of complex chemical reactions [7]. During hydrogen abstraction and recombination of the hydrogen atoms, exothermic reactions release energy which will locally recrystallize the amorphous phase. A continuous bombardment of atomic hydrogen and a supply of energy at the surface create local conditions under which an $sp^2$-bonded structure will be transformed into a relatively more stable network of $sp^3$-bonded carbon structure [12–14]. The disorder nano-domain has been reported to have $sp^3$ bonding [12–14]. Similarly, the disorder nano-phase domain will also be transformed into diamond with $sp^3$ bonding by the localized thermodynamic conditions. Therefore, there is a continuous phase transition from unstable to metastable and finally to stable, i.e. $sp^1$ bonding (carbon clusters) $\rightarrow$ $sp^2$-bonded phase (graphite and amorphous carbon) $\rightarrow$ $sp^3$-bonded phase (disorder domain and diamond). Thus, once recrystallization takes place in the amorphous region, it will act as a nucleation site for the growth of a

diamond crystal. The rate of formation of the amorphous phase, the rate of recrystallization of amorphous phase, and the diffusion rate are interdependent, and control the growth of diamond. The density and morphology of diamond depend significantly upon the nucleation density of crystallization of the amorphous phase [10]. Once diamond nucleation starts, the carbon atoms will rearrange to have the minimum surface energy depending on the crystallographic planes of the diamond crystal.

The ratio of total surface energy to volume is the most important factor in determining the morphology of diamond at the nucleation stage. The octahedron crystal, which is composed of (1 1 1) crystallographic planes, has the lowest surface energy ratio (0.55059) compared with dodecahedron (1 1 0), cubo-octahedron (1 0 0, 1 1 1) and cube (1 0 0) having surface-free energies of 0.63115, 0.75286 and 1.0, respectively [17]. Therefore, an initially formed diamond crystal might be an octahedron, which is the favourable thermodynamic equilibrium shape. Another important factor in determining the growth morphology of diamond is the specific energy of each growing plane. The growth shape of a diamond crystal will be dependent on the relative growth rate of constituent crystallographic planes. Under certain conditions, a higher-index crystal plane having higher specific energy will generally have a higher growth rate [17].

The present results are also in accordance with Ostwald's Rule which states that, in the course of going from a non-equilibrium phase to a final equilibrium state, a system will pass stepwise through states of intermediate stability [18, 19]. As applied to vapour quenching, the rule suggests that the condensed material will first pass through an amorphous state resembling the liquid, and then through high-temperature crystalline phases, before coming to equilibrium.

From the above results, it is suggested that the nucleation and growth mechanism of the diamond grown by the HFCVD process involves the following steps (Fig. 8).

## Step I: Formation of carbon clusters

In the early stage of the synthesis of diamond, clusters of carbon atoms are formed on the substrate surface. Due to continuous bombardment of atomic hydrogen and energy supply, there will be a change in the bonding structure from $sp^1$ to $sp^2$ because of local thermal conditions.

## Step II: Conversion of $sp^1 \rightarrow sp^2 \rightarrow sp^3$ bonding

A continuous molecular rain of activated hydrocarbon and atomic hydrogen on the surface of the substrate will provide enough energy to convert the $sp^2$-bonded carbon atoms into a relatively stable network of $sp^3$-bonded carbon. In addition, the etching of unstable phases ($sp^1$ and $sp^2$) will compete with the etching of stable phase ($sp^3$). As the etching rate of unstable phases is ten times faster than that of a stable phase, there will be a continuous phase transition from the $sp^2 \rightarrow sp^3$-bonded carbon phase. Atomic hydrogen plays an important role in promoting this

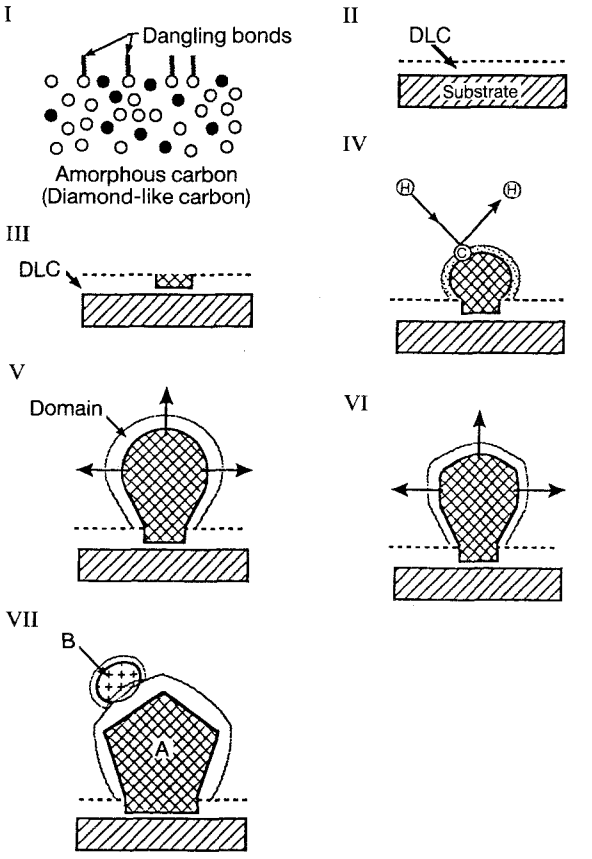


*Figure 8* Different steps involved during nucleation and growth of diamond crystal.

reaction and in stabilizing the phase. It was estimated that about 10 000 atomic hydrogen atoms must be produced for each carbon atom converted to $sp^s$ hybridization [8].

## Step III: Crystallization of amorphous phase

Crystallization in the amorphous layer will take place during the complex chemical reaction consisting of hydrogen abstraction, dehydrogenation of absorbed complexes, recombination of hydrogen atoms, etc. During or before the crystallization begins, there will be a transition of the bonding state of the carbon network from an amorphous phase with $sp^2$-bonded carbon, to disordered domain with $sp^3$-bonded carbon, to diamond with $sp^3$-bonded carbon. During the recrystallization process, the carbon atoms rearrange themselves to acquire minimum surface energy. The rearrangement of carbon atoms will be towards the (1 1 1) crystallographic plane of the diamond crystal, as it is with the lowest surface-free energy in the crystal [17]. The recrystallized regions will act as nuclei for the growth of diamond.

## Steps IV to VI: Growth of diamond crystal

During the diamond growth process, disordered domains of the diamond phase will always be a precursor for the growth of diamond. A cluster of carbon atoms with $sp^3$ bonding will be deposited on the surface of the precursor layer. These carbon atoms will diffuse inwards by a solid-state diffusion process [9]. The initial diamond shape will be hemispherical, as illustrated in Fig. 7. This figure corresponds to step IV of the proposed model as illustrated in Fig. 8. The exist-

ence of a hemispherical shape has been confirmed by examining a planar view of diamond growth on iron silicide [20]. Once the diamond has reached its critical size (step V), it will acquire a faceted crystallographic shape characterized by defects such as point defects, stacking faults and twins (step VI).

### Step VII: Secondary growth of diamond

Due to concentration fluctuations on the surface of diamond, the surface of the disordered domain will be uneven and, at the same time, the thickness of the domain will vary from 8–14 nm depending on the deposition conditions (Fig. 7). Once the thickness of the disordered domain exceeds the critical thickness ( > 15 nm), there will not be enough localized heat energy and time available to diffuse the carbon atoms into the diamond crystal. This additional build-up of amorphous layer will recrystallize by the mechanism proposed above. The secondary recrystallization will act as a nucleation site for the growth of secondary diamond on the primary diamond crystal. The amorphous layer will always exist initially between the primary diamond and secondary diamond crystallite. This will probably convert in the course of time, by atomic diffusion, to a diamond crystal, assuming a sufficient localized source of heat.

The present experimental observations support the fact that diamond growth is taking place by conversion of amorphous diamond-like carbon into diamond. According to the above models, available atomic hydrogen stabilizes $sp^3$ carbon bonds on the surface, and the growth of diamond occurs by replacing hydrogen by carbon. Further experiments are needed, however, to confirm this mechanism of diamond growth.

According to Fedoseev and Derjaguin [6], in the vicinity of a growing crystal surface there is a hyperconcentrated layer where homogeneous formation of nuclei and clusters of the new phase is possibly taking place, which is then incorporated into the lattice of the crystal. Thus surface diffusion is one of the rate-controlling steps for the growth of diamond. The surface diffusion and growth rate of diamond depend upon the deposition temperature. A correlation has been reported between surface morphology, defects and growth temperature. At higher deposition temperatures, the surface mobility of carbon atoms is increased, allowing the carbon atoms to rearrange themselves into their lowest equilibrium state prior to overgrowth. Therefore the atoms will incorporate into their correct lattice sites within 60° bond rotations, resulting in a (1 1 1) twin boundary or stacking fault [21].

## 5. Conclusions

The HRTEM micrographs show the presence of DLC or disorder domain of diamond around the diamond crystal. The domain surface was found to be uneven and the thickness of domain varied from 8–14 nm, depending on the thin-film deposition conditions. Small diamond crystallites were present in the amorphous diamond-like carbon which provided nucleation sites for the growth of diamond. A nucleation and growth model for diamond has been proposed in conjunction with the available theoretical models: step I, formation of carbon clusters; II, conversion of $sp^1 \rightarrow sp^2 \rightarrow sp^3$-bonded carbon atoms; III, crystallization of amorphous phase; IV, growth of diamond crystal. The surface diffusion of the carbon atoms is believed to be the rate-controlling step for the growth of diamond. The disorder domain or amorphous phase will always be a precursor layer for the growth of diamond.

**Acknowledgements**

Experimental work was performed at North Carolina State University, Raleigh, N.C. The author thanks M. Vellarkal, P. Tiwari, R. J. Nemanich and J. Narayan for their help and stimulating discussion.

## References

1. K. KOBASHI, K. NISHIMURA, Y. KAWATE and T. HORIUCHI, *Phys. Rev.* **38** (1988) 4067.
2. C. E. JOHNSON, W. A. WEIMER and F. M. CERIO, *J. Mater. Res.* **7** (1992) 1427.
3. L. R. MARTIN and M. W. HILL, *J. Mater. Sci. Lett.* **9** (1990) 621.
4. N. OHTAKE and M. YOSHIKAWA, *J. Electrochem. Soc.* **137** (1990) 717.
5. C. M. NIU, G. TSAGAROPOULOS, J. BAGLIO, K. DWIGHT and A. WOLD, *J. Solid State Chem.* **91** (1991) 47.
6. D. B. FEDOSEEV and B. V. DERJAGUIN, *Arch. Nauki Mater.* **7** (1986) 111.
7. M. FRENKLACH and K. E. SPEAR, *J. Mater. Res.* **3** (1988) 133.
8. T. R. ANTHONY, in "The Physics and Chemistry of Carbides, Nitrides and Borides" edited by R. Freer (Kluwer Academic Press Netherlands, 1989) p. 133.
9. B. LIU, G. S. SANDHU, N. R. PARIKH, M. L. SWANSON and W. K. CHU, *Nucl. Instr. Methods Phys. Res.* **B45** (1990) 420.
10. K. V. RAVI, C. A. KOCH, H. S. HU and A. JOSHI, *J. Mater. Res.* **5** 2357 (1990).
11. F. TUINSTA and J. L. KOENING, *J. Chem. Phys.* **53** (1970) 1126.
12. R. J. NEMANICH, L. BERGMAN, Y. M. LEGRICE and R. E. SHRODER, in Materials Research Society Proceeding of the International Conference on "New Diamond Science & Technology", edited by R. Messier, J. T. Glass, J. E. Butler and R. Roy (Materials Research Society, Pittsburgh, PA, 1990).
13. R. J. NEMANICH, J. T. GLASS, G. LUCOVSKY and R. E. SHRODER, *J. Vac. Sci. Tech.* **A6** (1988) 1783.
14. R. J. NEMANICH, R. E. SHRODER J. T. GLASS and G. LUCOVSKY, in Proceedings of the 19th International Conference on the Physics of Semiconductors edited by W. Zowadski (Institute of Physics, Polish Academy of Science, Warsaw, 1988) p. 515.
15. S. A. SOLIN and R. J. KOBLISKA, in "Amorphous and Liquid Semiconductors" edited by J. Stuke (Taylor & Francis, London, 1974) p. 1251.
16. R. E. SHRODER, R. J. NEMANICH and J. T. GLASS, *Phys. Rev. B* **41** (1990) 3738.
17. J. S. KIM, M. H. KIM, S. S. PARK and J. Y. LEE, *J. Appl. Phys.* **67** (1990) 33354.
18. W. OSTWALD, *Z. Physik Chem.* **22** (1897) 287.
19. A. S. NOWICK, *Comm. Solid State Phys.* **2** (1969) 155.
20. J. SINGH and M. VELLAIKAL, *Surf. coat. Tech.* (to be published).
21. G. H. M. MA, B. E. WILLIAMS, J. T. GLASS and J. T. PRATER, *Diamond Rel. Mater.* **1** (1991) 25.

*Received 16 September 1992*
*and accepted 27 September 1993*